Accepted version of the article published in IEEE Wireless Communications Letters, 2025. DOI: 10.1109/LWC.2025.3611843.
Available at http://ieeexplore.ieee.org

On the Solution to a Class of Multi-Functional Beamforming Problems

Jordi Borras, *Member, IEEE*, Andrea Guamo-Morocho, *Graduate Student Member, IEEE*, Nuria González-Prelcic, *Fellow, IEEE*, and Roberto López-Valcarce, *Senior Member, IEEE*

***Abstract*—Many emerging wireless applications require the simultaneous execution of multiple functions, such as information transmission and reception, or communication and sensing. This has driven the study of different means to optimize performance tradeoffs. Among these, the design of multi-functional beamformers often involves nonconvex quadratically constrained quadratic programs (QCQPs), which are commonly approached via semidefinite relaxation (SDR). Two well-known issues affecting the SDR approach are its tightness and the ability to extract a QCQP-feasible solution from the SDR solution. In this context, we identify a sufficient condition for strong duality of a class of nonconvex QCQPs, in which case the exact optimal solution can be readily obtained. The applicability of the proposed framework to the design of multi-functional beamformers is illustrated.**

***Index Terms*—Multi-functional beamforming, integrated sensing and communication, in-band full-duplex communications, self-interference cancellation.**

I. INTRODUCTION

MULTI-FUNCTIONAL beamforming has arisen as a key enabler for a range of applications envisioned for next-generation wireless networks involving the coexistence of several subsystems [1–3]. In essence, a beamformer is designed to either maximize a quality-of-service (QoS) metric for one subsystem, or to minimize the interference induced on one or several subsystems, while guaranteeing certain performance requirements for the remaining ones.

An application example is the underlay paradigm in cognitive radio networks: a secondary transmitter adjusts its beampattern to maximize the secondary network rate while limiting its interference to primary users [4], [5]. Another example is in-band full-duplex (IBFD) communication [6], where transmission and reception occur simultaneously and on the same frequency. This results in self-interference (SI) caused by leakage of transmitted signals on the co-located receiver. Transmit beamforming has emerged as an effective means to manage SI, either by imposing maximum SI constraints [7–9] while maximizing QoS, or by minimizing SI impact [10–12] under a minimum QoS requirement.

Work funded by MICIU/AEI/10.13039/501100011033 and by ERDF/EU under grants PID2022-136512OB-C21/C22 and fellowship PRE2020-096625 "ESF Investing in your future", and by grant 2021 SGR 01033.

J. Borras was with the atlanTTic Research Center, Universidade de Vigo, 36310 Vigo, Spain. He is now with the Department of Signal Theory and Communications, Universitat Politècnica de Catalunya, 08034 Barcelona, Spain. E-mail: jordi.borras@ieee.org

A. Guamo-Morocho and R. López-Valcarce are with the atlanTTic Research Center, Universidade de Vigo, 36310 Vigo, Spain. E-mail: aguamo@gts.uvigo.es, valcarce@gts.uvigo.es.

N. González-Prelcic is with the Electrical and Computer Engineering Department, University of California at San Diego, La Jolla, CA 92093 USA. E-mail: ngprelcic@ucsd.edu.

In the area of integrated sensing and communication (ISAC) [13], conventional approaches to enable both functionalities include convex combinations of sensing- and communication-optimal beamformers [14], which need not yield globally optimal solutions; or mixing radar and communication signaling [15], which requires interference cancellation at receivers. Multi-functional beamforming provides global solutions that may improve the communication-sensing tradeoff [16–19], and can also mitigate SI in monostatic ISAC systems [20–23].

Many multi-functional beamforming problems fall under the class of nonconvex quadratically constrained quadratic problems (QCQPs). These are typically transformed into rank-constrained semidefinite programs (SDPs) and approached via the semidefinite relaxation (SDR) method [24], which may not be tight, meaning that SDR only provides an approximate solution to the original nonconvex QCQP. Even in situations for which the SDR is tight, this only guarantees that the solution to the original QCQP is in the solution set of the relaxed problem; the SDR solution obtained by a convex solver may not be QCQP-feasible [25], and additional procedures may be needed to extract a feasible (and in general suboptimal) component from the SDR solution, making this approach computationally onerous. In this vein, [26] shows that any QCQP with at most three quadratic constraints admits a tight SDR. In such cases, the optimal QCQP-feasible solution can be recovered directly via [26, Algorithm 1]. However, this fundamental condition can be overly restrictive for some practical problems. In this context, we investigate a class of nonconvex, homogeneous QCQPs with an arbitrary number of inequality constraints. For these, we identify in Sec. II a sufficient condition on the solution of the corresponding dual problem for strong duality, in which case it also provides the optimal solution to the original QCQP. Thus, checking this condition before attempting to solve the corresponding SDR becomes appealing for problems in which the number of variables is much larger than the number of constraints. Examples in the context of IBFD and ISAC beamforming design are provided in Sec. III.

II. MAIN RESULT

Let $\boldsymbol{A}$ be an $n \times n$ Hermitian (possibly non-definite) matrix, and $\{\boldsymbol{B}_p\}_{p=1}^P$, $\{\boldsymbol{C}_q\}_{q=1}^Q$ be positive semidefinite $n\times n$ matrices. Consider the following homogeneous QCQP:

$$\min_{\boldsymbol{f}\in\mathbb{C}^n} \quad \boldsymbol{f}^H\boldsymbol{A}\boldsymbol{f} \tag{1a}$$

$$\text{s. t.} \quad \boldsymbol{f}^H\boldsymbol{B}_p\boldsymbol{f} \geq \tau_p^2, \quad p=1,\ldots,P, \tag{1b}$$

$$\boldsymbol{f}^H\boldsymbol{C}_q\boldsymbol{f} \leq \delta_q^2, \quad q=1,\ldots,Q, \tag{1c}$$

where $\tau_p^2 > 0$, $\delta_q^2 > 0$ for all p, q. Note that (1) is not convex unless $\boldsymbol{A} \succeq \boldsymbol{0}$ and $P = 0$. Typically, $\boldsymbol{f}$ is the beamforming vector, (1b) are related to beamforming gain in certain directions, and (1c) include interference and/or transmit power constraints. The following assumption will be adopted:

Assumption 1. *If $\boldsymbol{C}_q\boldsymbol{v} = \boldsymbol{0}$ simultaneously holds for all $q = 1, \ldots, Q$, then $\boldsymbol{v} = \boldsymbol{0}$.*

Assumption 1 makes sense in practice, because without it there would exist some subspace in which the transmit power remained unconstrained. Our main result is as follows:

Theorem 1. *Assume* (1) *is feasible and Assumption 1 holds. Let $\{\mu_{\star,p}\}$, $\{\eta_{\star,q}\}$ be a solution to the convex problem (SDP)*

$$\max_{\substack{\mu_1,\ldots,\mu_P \geq 0 \\ \eta_1,\ldots,\eta_Q \geq 0}} \quad \sum_{p=1}^{P} \mu_p \tau_p^2 - \sum_{q=1}^{Q} \eta_q \delta_q^2 \tag{2a}$$

$$\text{s. t.} \quad \boldsymbol{A} - \sum_{p=1}^{P} \mu_p \boldsymbol{B}_p + \sum_{q=1}^{Q} \eta_q \boldsymbol{C}_q \succeq \boldsymbol{0}. \tag{2b}$$

If the zero eigenvalue of the positive semidefinite matrix

$$\boldsymbol{H}_\star = \boldsymbol{A} - \sum_{p=1}^{P} \mu_{\star,p} \boldsymbol{B}_p + \sum_{q=1}^{Q} \eta_{\star,q} \boldsymbol{C}_q \tag{3}$$

is unique, i.e.*, it has multiplicity one, then the solution to* (1) *is given by $\boldsymbol{f}_\star = \alpha \boldsymbol{v}_\star$, where $\boldsymbol{v}_\star$ is the unit-norm least eigenvector of $\boldsymbol{H}_\star$, and*

$$\alpha^2 = \frac{\sum_{p=1}^{P} \mu_{\star,p} \tau_p^2 - \sum_{q=1}^{Q} \eta_{\star,q} \delta_q^2}{\boldsymbol{v}_\star^H \boldsymbol{A} \boldsymbol{v}_\star}. \tag{4}$$

Proof: Let $\boldsymbol{\mu} = [\,\mu_1 \cdots \mu_P\,]^T$, $\boldsymbol{\eta} = [\,\eta_1 \cdots \eta_Q\,]^T$ comprise the (nonnegative) Lagrange multipliers for problem (1), and let

$$\boldsymbol{H}(\boldsymbol{\mu}, \boldsymbol{\eta}) \triangleq \boldsymbol{A} - \sum_{p=1}^{P} \mu_p \boldsymbol{B}_p + \sum_{q=1}^{Q} \eta_q \boldsymbol{C}_q. \tag{5}$$

Then, the Lagrangian for problem (1) can be written as

$$\mathcal{L}(\boldsymbol{f}, \boldsymbol{\mu}, \boldsymbol{\eta}) = \boldsymbol{f}^H \boldsymbol{H}(\boldsymbol{\mu}, \boldsymbol{\eta}) \boldsymbol{f} + \sum_{p=1}^{P} \mu_p \tau_p^2 - \sum_{q=1}^{Q} \eta_q \delta_q^2, \tag{6}$$

and the corresponding dual function is

$$g(\boldsymbol{\mu}, \boldsymbol{\eta}) = \inf_{\boldsymbol{f}} \mathcal{L}(\boldsymbol{f}, \boldsymbol{\mu}, \boldsymbol{\eta}) \tag{7}$$

$$= \begin{cases} \sum_{p=1}^{P} \mu_p \tau_p^2 - \sum_{q=1}^{Q} \eta_q \delta_q^2, & \boldsymbol{H}(\boldsymbol{\mu}, \boldsymbol{\eta}) \succeq \boldsymbol{0}, \\ -\infty, & \text{otherwise}. \end{cases} \tag{8}$$

For all $\boldsymbol{\mu} \geq 0$, $\boldsymbol{\eta} \geq 0$, the dual function lower bounds the objective of the primal problem over the feasible set [27, Ch. 5]; the largest such bound is the solution to the dual problem, which is (2). Letting $\tilde{g}(\boldsymbol{\mu}, \boldsymbol{\eta}) \triangleq \sum_{p=1}^{P} \mu_p \tau_p^2 - \sum_{q=1}^{Q} \eta_q \delta_q^2$, the dual problem (which is convex) can be rewritten as

$$\max_{\boldsymbol{\mu} \geq 0, \boldsymbol{\eta} \geq 0} \; \tilde{g}(\boldsymbol{\mu}, \boldsymbol{\eta}) \quad \text{s. t.} \quad \lambda_{\min}\left(\boldsymbol{H}(\boldsymbol{\mu}, \boldsymbol{\eta})\right) \geq 0. \tag{9}$$

Note that Assumption 1 implies that $\sum_{q=1}^{Q} \eta_q \boldsymbol{C}_q$ is positive definite if $\eta_q > 0$ for all q. This, in turn, implies that (9) is strictly feasible: if we take $\boldsymbol{\mu} = \boldsymbol{1}$ (the all-ones vector) and $\boldsymbol{\eta} = \beta \boldsymbol{1}$, then $\boldsymbol{H}(\boldsymbol{1}, \beta \boldsymbol{1})$ will be positive definite for $\beta > \rho(\boldsymbol{A} - \sum_p \boldsymbol{B}_p)/\lambda_{\min}(\sum_q \boldsymbol{C}_q)$, where $\rho(\cdot)$ denotes the spectral radius. Hence, Slater's constraint qualification holds, and since (9) is convex, the Karush-Kuhn-Tucker (KKT) conditions must hold at any optimal solution $(\boldsymbol{\mu}_\star, \boldsymbol{\eta}_\star)$ [27, Ch. 5]. If the smallest eigenvalue of $\boldsymbol{H}_\star \triangleq \boldsymbol{H}(\boldsymbol{\mu}_\star, \boldsymbol{\eta}_\star)$ is unique, by direct application of the KKT conditions, there must exist a scalar $\alpha^2 \geq 0$ satisfying (10)-(11) at the bottom of this page.

We invoke now the following result [28]: for $\boldsymbol{M}$ Hermitian depending on $\theta \in \mathbb{R}$, if its i-th eigenvalue λ_i is unique, then

$$\frac{\partial \lambda_i}{\partial \theta} = \boldsymbol{v}_i^H \left(\frac{\partial \boldsymbol{M}}{\partial \theta} \right) \boldsymbol{v}_i, \tag{12}$$

where $\boldsymbol{v}_i$ is the unit-norm eigenvector of $\boldsymbol{M}$ associated to λ_i. Using this and the uniqueness of $\lambda_{\min}(\boldsymbol{H}_\star)$, (10)-(11) read as

$$\alpha^2 \boldsymbol{v}_\star^H \boldsymbol{B}_p \boldsymbol{v}_\star \begin{cases} = \tau_p^2, & \forall p \text{ such that } \mu_{\star,p} > 0, \\ \geq \tau_p^2, & \forall p \text{ such that } \mu_{\star,p} = 0, \end{cases} \tag{13}$$

$$\alpha^2 \boldsymbol{v}_\star^H \boldsymbol{C}_q \boldsymbol{v}_\star \begin{cases} = \delta_q^2, & \forall q \text{ such that } \eta_{\star,q} > 0, \\ \leq \delta_q^2, & \forall q \text{ such that } \eta_{\star,q} = 0, \end{cases} \tag{14}$$

where $\boldsymbol{v}_\star$ denotes the unit-norm least eigenvector of $\boldsymbol{H}_\star$. Then

$$\alpha^2 \lambda_{\min}(\boldsymbol{H}_\star) = \alpha^2 \boldsymbol{v}_\star^H \boldsymbol{H}_\star \boldsymbol{v}_\star \tag{15}$$

$$= \alpha^2 \boldsymbol{v}_\star^H \boldsymbol{A} \boldsymbol{v}_\star - \sum_{p=1}^{P} \mu_{\star,p} \tau_p^2 + \sum_{q=1}^{Q} \eta_{\star,q} \delta_q^2, \tag{16}$$

where (16) is due to (13)-(14) and the fact that $\mu_{\star,p} \geq 0$, $\eta_{\star,q} \geq 0$, $\forall p, q$. It follows from (16) that

$$\tilde{g}(\boldsymbol{\mu}_\star, \boldsymbol{\eta}_\star) + \alpha^2 \lambda_{\min}(\boldsymbol{H}_\star) = \alpha^2 \boldsymbol{v}_\star^H \boldsymbol{A} \boldsymbol{v}_\star. \tag{17}$$

Now note that $\lambda_{\min}(\boldsymbol{H}_\star)$ must be zero; otherwise, some entry of $\boldsymbol{\mu}_\star$ (resp. $\boldsymbol{\eta}_\star$) could be slightly increased (resp. decreased) so that the objective in (9) would increase without violating the constraints. Together with (17), this shows that

$$\sum_{p=1}^{P} \mu_{\star,p} \tau_p^2 - \sum_{q=1}^{Q} \eta_{\star,q} \delta_q^2 = \alpha^2 \boldsymbol{v}_\star^H \boldsymbol{A} \boldsymbol{v}_\star, \tag{18}$$

which equals the value of primal objective when evaluated at $\alpha \boldsymbol{v}_\star$. In addition, (13)-(14) show that $\alpha \boldsymbol{v}_\star$ is primal feasible. Hence, the duality gap is zero, and $\boldsymbol{f} = \alpha \boldsymbol{v}_\star$ is primal optimal. The value of α can be determined from (18), which yields (4).

$$\left. \frac{\partial(\tilde{g}(\boldsymbol{\mu}, \boldsymbol{\eta}) + \alpha^2 \lambda_{\min}(\boldsymbol{H}(\boldsymbol{\mu}, \boldsymbol{\eta})))}{\partial \mu_p} \right|_{(\boldsymbol{\mu}_\star, \boldsymbol{\eta}_\star)} \begin{cases} = 0, & \forall p \text{ such that } \mu_{\star,p} > 0, \\ \leq 0, & \forall p \text{ such that } \mu_{\star,p} = 0, \end{cases} \tag{10}$$

$$\left. \frac{\partial(\tilde{g}(\boldsymbol{\mu}, \boldsymbol{\eta}) + \alpha^2 \lambda_{\min}(\boldsymbol{H}(\boldsymbol{\mu}, \boldsymbol{\eta})))}{\partial \eta_q} \right|_{(\boldsymbol{\mu}_\star, \boldsymbol{\eta}_\star)} \begin{cases} = 0, & \forall q \text{ such that } \eta_{\star,q} > 0, \\ \leq 0, & \forall q \text{ such that } \eta_{\star,q} = 0. \end{cases} \tag{11}$$

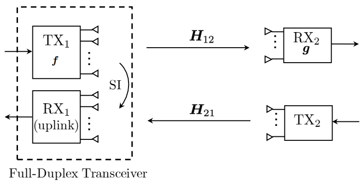

(a) Full-duplex communication architecture (Sec. III-A).

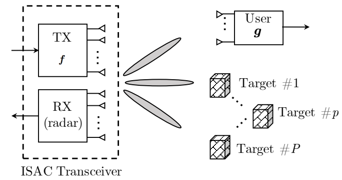

(b) Joint communication and sensing architecture (Sec. III-B).

Fig. 1: System model for the application examples discussed in Sec. III.

Note that (13)-(14) imply

$$\min_{1\leq q\leq Q}\left\{\frac{\delta_q^2}{\boldsymbol{v}_\star^H\boldsymbol{C}_q\boldsymbol{v}_\star}\right\}\geq\max_{1\leq p\leq P}\left\{\frac{\tau_p^2}{\boldsymbol{v}_\star^H\boldsymbol{B}_p\boldsymbol{v}_\star}\right\}. \tag{19}$$

A contradiction would arise if (19) did not hold, indicating that the primal problem, *i.e.,* the QCQP (1), is unfeasible. ■

Corollary 1. *Under the conditions of Theorem 1, the SDR of the QCQP* (1) *is tight.*

Proof: By Theorem 1, problem (1) enjoys strong duality. Now note that since Slater's constraint qualification applies to the (convex) dual problem (2), it also enjoys strong duality [27]. The dual of (2), *i.e.,* the bidual of (1), is the SDR of the original QCQP (1) [29]; hence, the optimal value of the SDR is equal to the optimal value of (1). ■

Computational complexity. The complexity of solving an SDP with c constraints and v variables via an interior point method (IPM) is roughly $\mathcal{O}((\max\{c,v\})^4)$ [24], [30]. Thus, solving (2) has complexity $\mathcal{O}((P+Q)^4)$, whereas checking the dimension of the null space of $\boldsymbol{H}_\star$ via Gaussian elimination has complexity $\mathcal{O}(n^3)$. In contrast, and assuming $n\geq P+Q$ as it is typically the case, the complexity of solving the SDR of (1) is $\mathcal{O}(n^4)$. Thus, for settings in which n is large, checking for strong duality via Theorem 1 may be appealing.

III. Examples

A. SI Cancellation (SIC) in Full-Duplex Communications

Fig. 1(a) shows an FD transceiver with separate, co-located transmit (TX) and receive (RX) arrays simultaneously performing uplink (TX$_2$ $\rightarrow$ RX$_1$) and downlink (TX$_1$ $\rightarrow$ RX$_2$) communication. Let N_i (resp. M_j) be the number of antennas at TX$_i$ (resp. RX$_j$). TX$_1$ employs a beamformer $\boldsymbol{f}\in\mathbb{C}^{N_1}$ to send a zero-mean, unit-variance symbol s through channel $\boldsymbol{H}_{12}\in\mathbb{C}^{M_2\times N_1}$. At RX$_2$, a beamformer $\boldsymbol{g}\in\mathbb{C}^{M_2}$ is applied, so that the received signal reads as

$$y=\boldsymbol{g}^H\boldsymbol{H}_{12}\boldsymbol{f}s+\boldsymbol{g}^H\boldsymbol{w}, \tag{20}$$

where $\boldsymbol{w}\sim\mathcal{N}_\mathbb{C}(\boldsymbol{0},\sigma^2\boldsymbol{I}_{M_2})$ is the thermal noise. Under this model, it is readily seen that the optimal RX beamformer is a maximal ratio combiner (MRC), *i.e.,* $\boldsymbol{g}=\boldsymbol{H}_{12}\boldsymbol{f}/\|\boldsymbol{H}_{12}\boldsymbol{f}\|$.

Since TX$_1$ and RX$_1$ are co-located, the downlink transmission causes SI in the FD receive array, which may severely degrade uplink performance. Among the different means to deal with SI, TX beamforming is appealing due to its capability to avoid saturation of the RX RF front-end. The goal is to minimize the SI power leaked on the RX array while guaranteeing a minimum beamforming gain for downlink communication, and under a total power constraint (TPC) or per-antenna power constraints (PAPC). Letting $\boldsymbol{H}_{\text{SI}}\in\mathbb{C}^{M_1\times N_1}$ be the SI channel matrix, the problem at hand can be formulated as

$$\min_{\boldsymbol{f}}\quad \boldsymbol{f}^H\boldsymbol{H}_{\text{SI}}^H\boldsymbol{H}_{\text{SI}}\boldsymbol{f} \tag{21a}$$

$$\text{s. t.}\quad \boldsymbol{f}^H\boldsymbol{H}_{12}^H\boldsymbol{H}_{12}\boldsymbol{f}\geq\tau^2 \tag{21b}$$

$$\begin{cases}\boldsymbol{f}^H\boldsymbol{f}\leq P_{\text{T}}, & \text{(TPC), or}\\ \boldsymbol{f}^H\boldsymbol{e}_i\boldsymbol{e}_i^H\boldsymbol{f}\leq p_i,\ i=1,\dots,N_1, & \text{(PAPC)}\end{cases} \tag{21c}$$

with $\boldsymbol{e}_i$ the i-th column of $\boldsymbol{I}_{N_1}$, τ^2 the minimum downlink gain, P_{T} the maximum total TX power, and p_i the maximum available power at the i-th antenna, satisfying $\sum_{i=1}^{N_1}p_i=P_{\text{T}}$. Note, (21) has the same structure as (1) with $\boldsymbol{A}=\boldsymbol{H}_{\text{SI}}^H\boldsymbol{H}_{\text{SI}}$, $P=1$, $\boldsymbol{B}_1=\boldsymbol{H}_{12}^H\boldsymbol{H}_{12}$, and $(Q=1,\boldsymbol{C}_1=\boldsymbol{I}_{N_1})$ for TPC or $\left(Q=N_1,\boldsymbol{C}_q=\boldsymbol{e}_q\boldsymbol{e}_q^H\right)$ for PAPC.

The application of Theorem 1 to (21) is tested in this scenario, assuming half-wavelength uniform linear arrays (ULAs) with $N_1=16$, $M_1=M_2=8$. For the downlink channel we adopt the narrowband clustered model [31]:

$$\boldsymbol{H}_{12}=\sum_{m=1}^{N_{\text{cl}}}\sum_{n=1}^{N_{\text{ray}}}g_{mn}\boldsymbol{a}_{\text{R}}\left(\theta_{mn}\right)\boldsymbol{a}_{\text{T}}^H\left(\phi_{mn}\right), \tag{22}$$

with N_{cl} and N_{ray} the number of clusters and of rays per cluster, resp., and g_{mn}, ϕ_{mn}, and θ_{mn} the complex gain, angle of departure (AoD), and angle of arrival (AoA) for the n-th ray in the m-th cluster. $\boldsymbol{a}_{\text{T}}(\phi)$ and $\boldsymbol{a}_{\text{R}}(\theta)$ are the steering vectors corresponding to the TX and RX arrays. Regarding the SI channel, $\boldsymbol{H}_{\text{SI}}\in\mathbb{C}^{M_1\times N_1}$ captures two effects: the near-field coupling and the far-field reflections due to nearby scatterers. Following [21], [31], the near-field term is modeled as

$$[\boldsymbol{H}_{\text{NF}}]_{pq}=\frac{1}{d_{pq}}e^{-\jmath 2\pi d_{pq}/\lambda}, \tag{23}$$

with λ the wavelength and d_{pq} the distance between the p-th TX and q-th RX antennas. The far-field term $\boldsymbol{H}_{\text{FF}}$ follows (22). Both terms are normalized so that $\|\boldsymbol{H}_{\text{FF}}\|_{\text{F}}^2=\|\boldsymbol{H}_{\text{NF}}\|_{\text{F}}^2=N_1M_1$. Then, for a given Rice factor κ, $\boldsymbol{H}_{\text{SI}}$ is given by

$$\boldsymbol{H}_{\text{SI}}=\sqrt{\frac{\kappa}{\kappa+1}}\boldsymbol{H}_{\text{NF}}+\sqrt{\frac{1}{\kappa+1}}\boldsymbol{H}_{\text{FF}}. \tag{24}$$

We consider $N_{\text{cl}}=4$ and $N_{\text{ray}}=8$ for all links, and $\kappa=10$ dB. AoDs/AoAs are Gaussian with standard deviation of $8°$ and mean cluster angles uniformly distributed within $[0,360°]$. Path gains are i.i.d. complex Gaussian with mean 1 dB and standard deviation 0.5 dB. Array geometry is as in [31, Fig. 2], with $\alpha=\beta=\frac{\pi}{2}$ and $\delta=2\lambda$. Channel matrices are normalized so that $\|\boldsymbol{H}_{12}\|_{\text{F}}^2=N_1M_2$ and $\|\boldsymbol{H}_{\text{SI}}\|_{\text{F}}^2=N_1M_1$. The minimum downlink beamforming gain is set as $\tau^2=\gamma\lambda_{\max}(\boldsymbol{H}_{12}^H\boldsymbol{H}_{12})$, with $\gamma\in[0,1]$, whereas power constraints are set as $P_{\text{T}}=1$ (TPC) and $p_1=\cdots=p_{N_1}=\frac{1}{N_1}$ (PAPC).

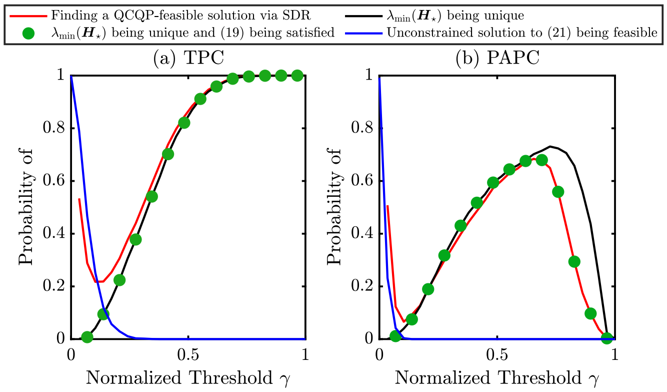

Fig. 2: Probabilistic analysis of problem (21).

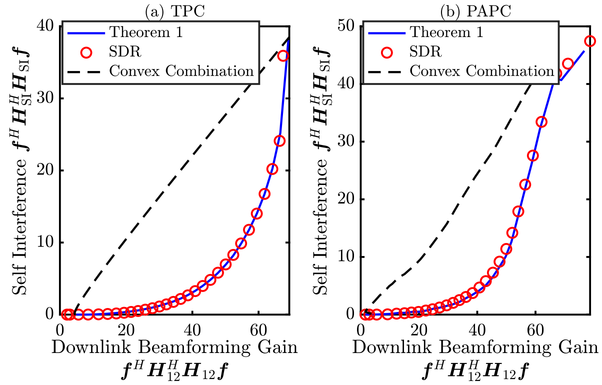

Fig. 3: Tradeoff curves for problem (21) sweeping γ from 0 to 1.

In Fig. 2 we compare, in a probabilistic sense, the outcomes of attempting to solve (21) via Theorem 1, or directly applying SDR to (21), in which case the rank-1 candidate solution is taken as the principal eigenvector (no improvement was observed by using randomization). In all cases, we first checked if a feasible vector in the null space of $\boldsymbol{H}_{\mathrm{SI}}^H\boldsymbol{H}_{\mathrm{SI}}$ exists (termed "unconstrained solution" in Fig. 2).

TPC case: The SDR of (21) is always tight, since the number of constraints is no more than three [24]; however, the adopted IPM is not guaranteed to find the rank-1 solution. Although (21) is always feasible under TPC for $P_{\mathrm{T}} = 1$ and $\gamma \in [0, 1]$, the rank-1 component extracted from the SDR solution may turn out to be unfeasible, see Fig. 2(a). It was observed that when constraint (21b) is loose (small γ), the IPM tends to find high-rank solutions, and the probability of extracting a feasible rank-1 solution drops for $\gamma \approx 0.15$. As γ increases, the IPM is more likely to find rank-1 solutions, which are optimal since SDR is tight. As seen in Fig. 2(a), whenever $\lambda_{\min}(\boldsymbol{H}_\star)$ is unique, (19) holds, as expected since (21) is always feasible. Note that, in this case, a rank-1 solution can always be found via [26, Algorithm 1]. However, when $\lambda_{\min}(\boldsymbol{H}_\star)$ is unique, Theorem 1 permits finding the optimal solution with much less computational cost.

PAPC case: Under PAPC, (21) may or may not be feasible depending on the value of γ. Now the number of constraints is $P + Q = N_1 + 1$, and the SDR of (21) need not be tight if $N_1 > 2$. As seen in Fig. 2(b), there exist cases in which (19) is not satisfied although $\lambda_{\min}(\boldsymbol{H}_\star)$ is unique, pointing to primal infeasibility, more likely as $\gamma \to 1$.

Fig. 3 shows the corresponding tradeoff curves for both approaches, together with that based on a convex combination (CC) of SIC-only and communication-only solutions[1] (which is analogous to multibeam designs for joint communication and sensing [32], [33]). It is seen that, whenever a feasible rank-1 solution is found from SDR and $\lambda_{\min}(\boldsymbol{H}_\star)$ happens to be unique, both approaches yield the same solution in this setting, both under TPC and PAPC; whereas the CC approach suffers a significant loss.

[1]The SIC-only solution $\boldsymbol{f}_{\mathrm{SIC}}$ is given by the least eigenvector of $\boldsymbol{H}_{\mathrm{SI}}^H\boldsymbol{H}_{\mathrm{SI}}$, whereas the communication-only solution $\boldsymbol{f}_{\mathrm{com}}$ is the principal eigenvector of $\boldsymbol{H}_{12}^H\boldsymbol{H}_{12}$. Then, the CC solution reads as $\boldsymbol{f}_{\mathrm{CC}} = (1-\omega)\boldsymbol{f}_{\mathrm{SIC}} + \omega\boldsymbol{f}_{\mathrm{com}}$, with $\omega \in [0, 1]$, which may need to be (element-wise) scaled to satisfy TPC/PAPC.

B. Integrated Sensing and Communication under PAPC

Consider now the setting from Fig. 1(b), in which an ISAC transceiver, equipped with an array of N_{T} antennas, simultaneously performs downlink single-stream communication and radar sensing toward P targets. It transmits a zero-mean, unit-variance symbol s to the downlink user, which has an array of M_{U} antennas. Letting $\boldsymbol{f} \in \mathbb{C}^{N_{\mathrm{T}}}$, $\boldsymbol{g} \in \mathbb{C}^{M_{\mathrm{U}}}$ and $\boldsymbol{H}_{\mathrm{c}} \in \mathbb{C}^{M_{\mathrm{U}} \times N_{\mathrm{T}}}$ be the TX and RX beamforming vectors and the downlink channel matrix, resp., the received signal reads analogously to (20). Again, MRC beamforming is optimal at RX: $\boldsymbol{g} = \boldsymbol{H}_{\mathrm{c}}\boldsymbol{f}/\|\boldsymbol{H}_{\mathrm{c}}\boldsymbol{f}\|$.

One possible design for the ISAC TX beamformer is to maximize the downlink beamforming gain under a requirement on the TX beampattern gain in the direction of each target. Under PAPC, this is formulated as

$$\min_{\boldsymbol{f}} \quad -\boldsymbol{f}^H\boldsymbol{H}_{\mathrm{c}}^H\boldsymbol{H}_{\mathrm{c}}\boldsymbol{f} \tag{25a}$$

$$\text{s. t.} \quad |\boldsymbol{f}^H\boldsymbol{a}_{\mathrm{T}}(\theta_p)|^2 \geq \tau_p^2, \; p = 1, \ldots, P, \tag{25b}$$

$$\boldsymbol{f}^H\boldsymbol{e}_q\boldsymbol{e}_q^H\boldsymbol{f} \leq p_q, \; q = 1, \ldots, N_{\mathrm{T}}, \tag{25c}$$

where τ_p^2 is the minimum gain in the direction of the p-th target. Note that (25) fits the general structure of (1), with $\boldsymbol{A} = -\boldsymbol{H}_{\mathrm{c}}^H\boldsymbol{H}_{\mathrm{c}}$, $\boldsymbol{B}_p = \boldsymbol{a}_{\mathrm{T}}(\theta_p)\boldsymbol{a}_{\mathrm{T}}^H(\theta_p)$, $\boldsymbol{C}_q = \boldsymbol{e}_q\boldsymbol{e}_q^H$, and $Q{=}N_{\mathrm{T}}$.

As in Sec. III-A, we assume a setting with $\frac{\lambda}{2}$-spaced ULAs, $N_{\mathrm{T}} = 16$, $M_{\mathrm{U}} = 8$, and $P = 2$ targets. The downlink channel $\boldsymbol{H}_{\mathrm{c}}$ is modeled as in (22) with the corresponding parameters given below (24). Target directions θ_p, $\forall p$, follow the same distribution as AoDs/AoAs. The channel matrix and steering vector are normalized so that $\|\boldsymbol{H}_{\mathrm{c}}\|_{\mathrm{F}}^2 = N_{\mathrm{T}}M_{\mathrm{U}}$ and $\|\boldsymbol{a}_{\mathrm{T}}(\theta)\|^2 = N_{\mathrm{T}}$. TX beampattern gain constraints are set to $\tau_p^2 = \gamma_p\lambda_{\max}(\boldsymbol{a}_{\mathrm{T}}(\theta_p)\boldsymbol{a}_{\mathrm{T}}^H(\theta_p))$, with $\gamma_p \in [0, 1]$, $\forall p$, and power constraints are set to $p_q = \frac{1}{N_{\mathrm{T}}}$, $\forall q$.

Numerical results are shown in Fig. 4. The CC solution is omitted since $P > 1$. Note that, since problem (25) has $P + N_1 > 3$ constraints, the SDR of (25) need not be tight. As in Sec. III-A, a rank-1 component from the SDR solution is extracted from the principal eigenvector, as no improvements were observed when using Gaussian randomization. As shown in Fig. 4, this rank-1 component slightly underperforms the optimal solution obtained via Theorem 1, while both approaches have the same worst-case complexity $\mathcal{O}((P + N_{\mathrm{T}})^4)$.

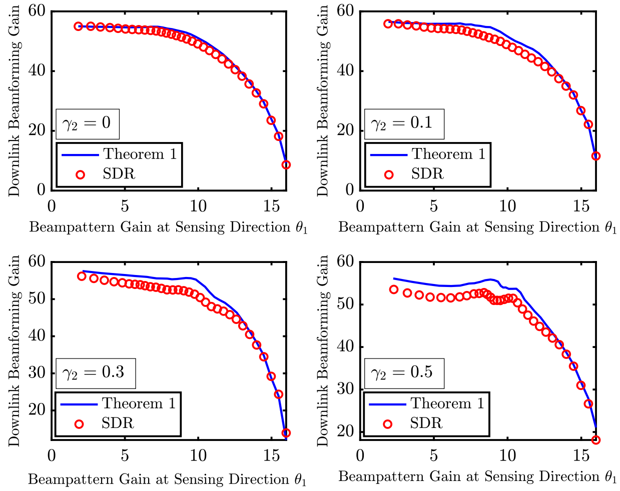

Fig. 4: Tradeoff curves between the downlink beamforming gain, *i.e.*, $\boldsymbol{f}^H \boldsymbol{H}_c^H \boldsymbol{H}_c \boldsymbol{f}$, and the beampattern gain at sensing direction θ_1, *i.e.*, $|\boldsymbol{f}^H \boldsymbol{a}_T(\theta_1)|^2$, for problem (25) (sweeping γ_1 from 0 to 1) under PAPC and fixed $\tau_2^2 = \gamma_2 \lambda_{\max}(\boldsymbol{a}_T(\theta_2)\boldsymbol{a}_T^H(\theta_2))$, with $\gamma_2 = \{0, 0.1, 0.3, 0.5\}$.

IV. Conclusions

Our analysis exposed a condition for strong duality of a class of QCQPs, and from which the optimal solution emerges. Fulfillment of this condition also implies SDR tightness. Since a rank-constrained solution may be hard to extract from the SDR solution, our result may be potentially useful in certain settings, especially if the number of variables is much larger than that of constraints.

References

[1] Z. Wei, F. Liu, C. Masouros, N. Su, and A. P. Petropulu, "Toward multi-functional 6G wireless networks: Integrating sensing, communication, and security," *IEEE Commun. Mag.*, vol. 60, no. 4, pp. 65–71, 2022.

[2] G. Caire, C. R. C. M. da Silva, T. Gu, and W. Yuan, "Integrating sensing into communications in multi-functional networks," *IEEE Commun. Mag.*, vol. 61, no. 5, pp. 24–25, 2023.

[3] Y. Zhao, Q. Wu, W. Chen, Y. Zeng, R. Liu, W. Mei, F. Hou, and S. Ma, "Multi-functional beamforming design for integrated sensing, communication, and computation," *IEEE Trans. Commun.*, vol. 73, no. 8, pp. 6322–6336, 2025.

[4] Y. Xu, X. Zhao, and Y.-C. Liang, "Robust power control and beamforming in cognitive radio networks: A survey," *IEEE Commun. Surveys Tut.*, vol. 17, no. 4, pp. 1834–1857, 2015.

[5] M. El Tanab and W. Hamouda, "Resource allocation for underlay cognitive radio networks: A survey," *IEEE Commun. Surveys Tut.*, vol. 19, no. 2, pp. 1249–1276, 2017.

[6] B. Smida, A. Sabharwal, G. Fodor, G. C. Alexandropoulos, H. A. Suraweera, and C.-B. Chae, "Full-duplex wireless for 6G: Progress brings new opportunities and challenges," *IEEE J. Sel. Areas Commun.*, vol. 41, no. 9, pp. 2729–2750, 2023.

[7] S. Huberman and T. Le-Ngoc, "MIMO full-duplex precoding: A joint beamforming and self-interference cancellation structure," *IEEE Trans. Wireless Commun.*, vol. 14, no. 4, pp. 2205–2217, 2015.

[8] N. M. Gowda and A. Sabharwal, "JointNull: Combining partial analog cancellation with transmit beamforming for large-antenna full-duplex wireless systems," *IEEE Trans. Wireless Commun.*, vol. 17, no. 3, pp. 2094–2108, 2018.

[9] X. Huang, A. Tuyen Le, and Y. J. Guo, "Transmit beamforming for communication and self-interference cancellation in full duplex MIMO systems: A trade-off analysis," *IEEE Trans. Wireless Commun.*, vol. 20, no. 6, pp. 3760–3769, 2021.

[10] I. T. Cummings, J. P. Doane, T. J. Schulz, and T. C. Havens, "Aperture-level simultaneous transmit and receive with digital phased arrays," *IEEE Trans. Signal Process.*, vol. 68, pp. 1243–1258, 2020.

[11] C. K. Sheemar and D. Slock, "Beamforming for bidirectional MIMO full duplex under the joint sum power and per antenna power constraints," in *IEEE Int. Conf. Acoust., Speech Signal Process. (ICASSP)*, 2021, pp. 4800–4804.

[12] A. Liu, W. Sheng, and T. Riihonen, "Per-antenna self-interference cancellation beamforming design for digital phased array," *IEEE Signal Process. Lett.*, vol. 29, pp. 2442–2446, 2022.

[13] F. Liu, Y. Cui, C. Masouros, J. Xu, T. X. Han, Y. C. Eldar, and S. Buzzi, "Integrated sensing and communications: Toward dual-functional wireless networks for 6G and beyond," *IEEE J. Sel. Areas Commun.*, vol. 40, no. 6, pp. 1728–1767, 2022.

[14] J. Suh, J. Kang, K. Han, S. Hong, and G.-T. Gil, "Null space projection-based design of multibeam for joint communication and sensing systems," *IEEE Commun. Lett.*, vol. 27, no. 8, pp. 2162–2166, 2023.

[15] H. Hua, J. Xu, and T. X. Han, "Optimal transmit beamforming for integrated sensing and communication," *IEEE Trans. Veh. Technol.*, vol. 72, no. 8, pp. 10 588–10 603, 2023.

[16] F. Liu, L. Zhou, C. Masouros, A. Li, W. Luo, and A. Petropulu, "Toward dual-functional radar-communication systems: Optimal waveform design," *IEEE Tran. Signal Process.*, vol. 66, no. 16, pp. 4264–4279, 2018.

[17] Y. Luo, J. A. Zhang, X. Huang, W. Ni, and J. Pan, "Multibeam optimization for joint communication and radio sensing using analog antenna arrays," *IEEE Trans. Veh. Technol.*, vol. 69, no. 10, pp. 11 000–11 013, 2020.

[18] N. Zhao, Y. Wang, Z. Zhang, Q. Chang, and Y. Shen, "Joint transmit and receive beamforming design for integrated sensing and communication," *IEEE Commun. Lett.*, vol. 26, no. 3, pp. 662–666, 2022.

[19] B. Liao, X. Xiong, and Z. Quan, "Robust beamforming design for dual-function radar-communication system," *IEEE Trans. Veh. Technol.*, vol. 72, no. 6, pp. 7508–7516, 2023.

[20] Z. Liu, S. Aditya, H. Li, and B. Clerckx, "Joint transmit and receive beamforming design in full-duplex integrated sensing and communications," *IEEE J. Sel. Areas Commun.*, vol. 41, no. 9, pp. 2907–2919, 2023.

[21] Z. He, W. Xu, H. Shen, D. W. K. Ng, Y. C. Eldar, and X. You, "Full-duplex communication for ISAC: Joint beamforming and power optimization," *IEEE J. Sel. Areas Commun.*, vol. 41, no. 9, pp. 2920–2936, 2023.

[22] M. T. Kabir, A. Gaydamaka, A. Mohammad, D. Moltchanov, and B. Tan, "The complete Pareto points for in-band full duplex integrated sensing and communication systems," *IEEE J. Sel. Areas Sensors*, vol. 1, pp. 198–210, 2024.

[23] M. Bayraktar, N. González-Prelcic, H. Chen, and C. J. Zhang, "Truly full-duplex integrated sensing and single-user communication at mmWave," in *IEEE Int. Workshop Signal Process. Adv. Wireless Commun. (SPAWC)*, 2024, pp. 116–120.

[24] Z.-Q. Luo, W.-K. Ma, A. M.-C. So, Y. Ye, and S. Zhang, "Semidefinite relaxation of quadratic optimization problems," *IEEE Signal Process. Mag.*, vol. 27, no. 3, pp. 20–34, 2010.

[25] Y. Ye. (1995) *Convergence behavior of central paths for convex homogeneous self–dual cones*. [Online]. Available: https://stanford.edu/%7Eyyye/yyye/ye.ps

[26] Y. Huang and D. P. Palomar, "Rank-constrained separable semidefinite programming with applications to optimal beamforming," *IEEE Trans. Signal Process.*, vol. 58, no. 2, pp. 664–678, 2010.

[27] S. Boyd and L. Vandenberghe, *Convex Optimization*. Cambridge University Press, 2004.

[28] N. P. van der Aa, H. G. ter Morsche, and R. M. Mattheij, "Computation of eigenvalue and eigenvector derivatives for a general complex-valued eigensystem," *Elec. J. Linear Algebra*, vol. 16, pp. 300–314, 2007.

[29] L. Vandenberghe and S. Boyd, "Semidefinite programming," *SIAM Rev.*, vol. 38, no. 1, pp. 49–95, 1996.

[30] L. Vandenberghe, V. R. Balakrishnan, R. Wallin, A. Hansson, and T. Roh, "Interior-point algorithms for semidefinite programming problems derived from the KYP lemma," in *Positive polynomials in control*. Springer, 2005, pp. 195–238.

[31] R. López-Valcarce and M. Martínez-Cotelo, "Full-duplex mmWave MIMO with finite-resolution phase shifters," *IEEE Trans. Wireless Commun.*, vol. 21, no. 11, pp. 8979–8994, 2022.

[32] A. Liu, T. Riihonen, and W. Sheng, "Full-duplex analog beamforming design for mm-Wave integrated sensing and communication," in *IEEE Radar Conf.*, 2023, pp. 1–6.

[33] M. Bayraktar, N. González-Prelcic, and H. Chen, "Hybrid precoding and combining for mmWave full-duplex joint radar and communication systems under self-interference," in *IEEE Int. Conf. Commun. (ICC)*, 2024, pp. 915–920.